

© 2004 Society of Photo-Optical Instrumentation Engineers.

This paper was published in SPIE Proceedings Volume 5362 and is made available as an electronic reprint with permission of SPIE. One print or electronic copy may be made for personal use only. Systematic or multiple reproduction, distribution to multiple locations via electronic or other means, duplication of any material in this paper for a fee or for commercial purposes, or modification of the content of the paper are prohibited.

Sorting through the lore of phase mask options – performance measures and practical commercial designs

Michael J. O’Callaghan*

Displaytech, Inc., 2602 Clover Basin Drive, Longmont, Colorado 80503

ABSTRACT

Phase masks are needed in Fourier-transform holographic data storage systems (HDS) to reduce the range of light intensities projected into the Fourier plane. The range of light intensities must match the dynamic range of the holographic storage medium and of the full HDS system. Descriptions, mathematical models, and tests of a variety of phase mask types have been reported in the literature: pixelated phase masks, non-pixelated phase masks, and axicons. Lacking, however, has been a systematic way of comparing the relative merits of phase mask types in order to make sound choices. To address this problem, performance criteria are proposed for both the Fourier plane and for the output image plane (e.g. the margin by which 1’s can be distinguished from 0’s). The criteria are useful both for comparisons and for design optimization. A new numerical model has been developed enabling quantitative comparisons to be made between the predicted performance of the various phase mask types. The model reported here enables more extensive investigations than could be carried out with previously reported models, including investigation of systems in which multiple bits of data are encoded by each pixel using light intensity modulation. The viability of using non-pixelated phase masks integrated with spatial light modulators is also examined. The use of non-pixelated (continuous random) phase masks instead of the more common pixelated phase masks would eliminate the need for costly precision lateral alignment, and integration eliminates the need for precise positioning in an image plane. These advantages would enable smaller, cheaper, high performance HDS optical systems.

Keywords: holographic data storage, spatial light modulator, phase mask

1. INTRODUCTION

Very early in the development of holographic data storage (HDS) it became apparent that system performance would be limited by storage media dynamic range. Phase masks were proposed as a means to even out the brightness distribution in the Fourier plane, thus relaxing storage media requirements¹. Since then a variety of phase mask types have been proposed and investigated²⁻¹⁶. Their effectiveness for re-distributing Fourier plane optical energy has been studied, as well as both the benefits and the adverse consequences for fidelity of recalled data pages^{13, 14, 17, 18}.

How can an HDS system designer go about selecting a type and design of phase mask? There is a substantial body of published work on particular types, but there has been no common measure that readily allows comparison of one type or design to another (although one author⁴ proposes a measurement that might be used for that purpose). Displaytech has undertaken development of spatial light modulators (SLMs used as write-heads in HDS systems) that will contain an integrated phase mask in order to support companies that are currently working to commercialize HDS technology¹⁹. Integration of the phase mask into the SLM shrinks the size of the HDS optical system and eliminates costly, high-precision opto-mechanics that is otherwise needed to accommodate a discrete phase mask; this makes the complete HDS drive both smaller and cheaper. How do we choose which type of phase mask to use with the SLM?

To help answer this question we have defined performance metrics for both the Fourier plane and the recalled image plane, and we’ve carried out numerical simulations of various phase masks to compute values for these metrics. In addition to computing metrics useful for comparing one phase mask to another, we’ve been able to combine metrics

* mikeo@displaytech.com; phone 1 303 774-2272; fax 1 303 772-2193; www.displaytech.com

to show that there is a tradeoff between data storage density and the degree of Fourier plane dynamic range reduction. Using the tools developed for this study, we've also carried out initial investigations into issues concerning the use of gray scale in SLMs (multiple brightness levels per pixel).

2. THE FOURIER PLANE PROBLEM

In holographic data storage systems an SLM is used as the write head that transforms electronic data into optical data. Most commonly, the 1's and 0's of a binary data set are represented by SLM pixels (Figure 1) that are either ON (transmissive) or OFF (opaque). Rather than directly storing an image of the SLM, typical HDS systems instead project the optical Fourier transform of the SLM image $\mathcal{F}[\text{SLM}]$ into the storage medium²⁰. The Fourier transform consists of a central (DC) spot representing the average brightness of all pixels in the SLM, plus a surrounding region (referred to as the AC portion) that contains information about the spatial distribution of ON and OFF pixels. For a typical data set in which roughly half of the pixels are ON and half are OFF, the ratio of the central spot's brightness to that of the surrounding region in the Fourier plane is proportional to N^2 for a two-dimensional SLM consisting of $N \times N$ pixels.

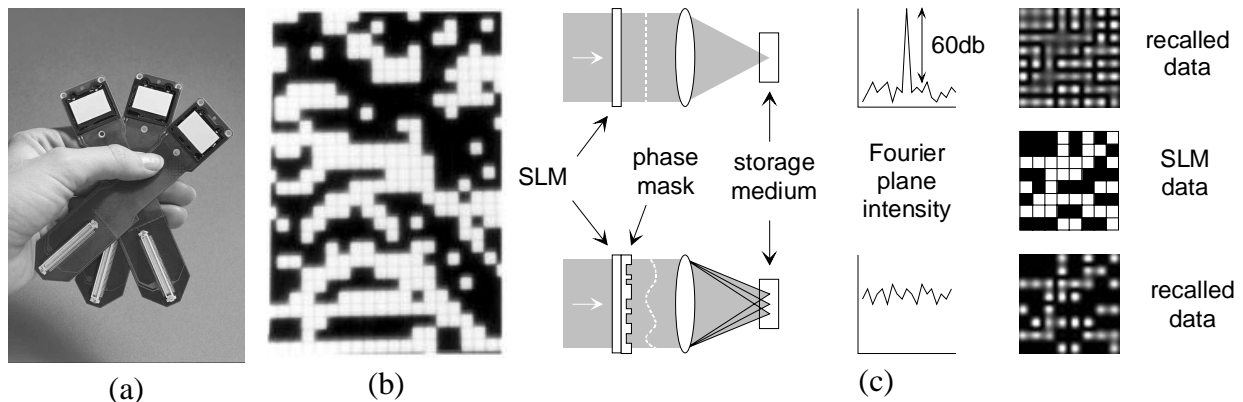


Figure 1. (a) Displaytech 1280×768 SLMs. (b) Photomicrograph of SLM pixels. (c) Simulated Fourier plane light intensity and recalled data without a phase mask (top) and with (bottom). The 60db “hot spot” (eliminated by the phase mask) is not reproduced on readout due to the storage medium’s finite dynamic range, thus degrading recalled data. For simplicity SLMs are shown here as transmissive instead of reflective, and the reference beam that interferes with the data beam within the storage medium is not shown.

For a 1000×1000 pixel SLM, the central DC spot of a typical data set’s Fourier transform will be on average 10^6 times brighter (60dB) than light in other parts of the Fourier transform. The problem is that it is difficult to accurately record and recall a wavefront having such an extreme dynamic range. The top portion of Figure 1(c) shows the simulation of a recalled SLM image in which the bright DC spot has been lost due to dynamic range limitations. The loss of DC information has made it virtually impossible to distinguish between ON and OFF pixels when detecting only the image’s brightness.

The job of the phase mask is to redistribute light from the 0-dimensional point-like DC spot into a broader 2-dimensional distribution, so that information about the DC part of the SLM has an amplitude that is more similar to the AC part (which in general is spread over a broad 2-dimensional area). The phase mask impresses a spatially varying phase on light leaving the SLM without affecting the brightness of the ON/OFF pixels; light in the Fourier plane then becomes a convolution of the transforms of the SLM and phase mask: $\mathcal{F}[\text{SLM}] * \mathcal{F}[\text{PM}]$. Convolution blurs the DC spot so that it occupies a much greater area, thus making it dimmer. The bottom portion of Figure 1(c) shows a simulation of the improvement in ON/OFF discrimination produced by a pixelated binary phase mask, the relative phase of each pixel has been randomly set to a value of 0 or π radians.

3. PHASE MASK TYPES

One way to implement a phase mask is to fabricate a window whose thickness $t_w(x,y)$ varies throughout the SLM aperture. The phase function for a window in air is $\phi(x,y) = 2\pi(n_w - 1)t_w(x,y)/\lambda$ where n_w is the window’s index of refraction. Three general classes of phase masks discussed in the literature are illustrated in Figure 2: pixelated^{1-3, 5, 6, 9,}

^{13-15, 17, 18}, non-pixelated^{5, 6, 9}, and axicons^{16, 20}. Axicons can be considered to be a special case of non-pixelated phase masks.

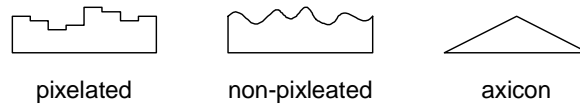


Figure 2. Illustration of pixelated, non-pixelated, and axicon phase masks.

In pixelated phase masks phase delays vary in discrete steps and are constant over an area of one or more SLM pixels. Non-pixelated phase masks have the virtue of not needing to be accurately aligned with pixels of the SLM, a property shared with conically shaped axicons.

The relative phase delays of individual pixels in a pixelated phase mask can be chosen randomly. However, choosing phase values without restriction enhances interpixel crosstalk in recalled images^{13, 17, 18}, thus degrading the distinction between ON and OFF pixels. This has led to the use of “pseudo-random” phase masks¹³ or to placing restrictions on allowable patterns of neighboring 1’s and 0’s^{17, 18}. In pseudo-random masks an upper limit is placed on the size of phase difference allowed between neighboring pixels, in effect limiting the spatial frequency content of the phase mask. We use the ratio Δ/π to characterize phase mask designs where Δ is the maximum allowed pixel-to-pixel phase change. In addition to being used for pixelated and non-pixelated phase masks we also use this ratio to characterize the phase slopes of axicons.

Examples of Fourier transforms of two phase masks types are shown in Figure 3. At left is the Fourier transform of a uniform window (i.e. no phase variations), in the center is the Fourier transform of an axicon, and at right is the transform of a pixelated random binary phase mask (phase delays of 0 and π). All of the Fourier transform energy of the uniform window is focused to a diffraction limited (0-dimensional) spot of light. Axicons redistribute light to fall within the diffraction limited width of the 1-dimensional curve of a circle. Pixelated and non-pixelated phase masks redistribute light to fall within a 2-dimensional area whose extent is dictated by the spatial frequency content of the phase mask.

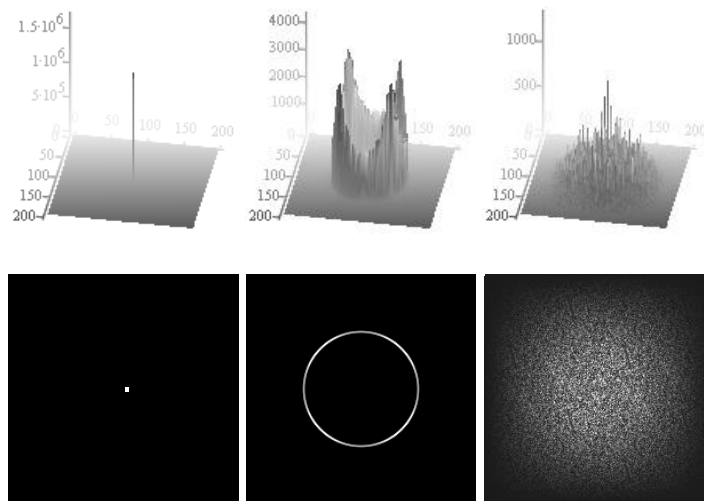


Figure 3. These plots show the $|\text{Fourier transforms}|^2$ of three types of phase mask for a 100×100 pixel SLM. Left: a uniform window (i.e. no phase mask). Center: an axicon. Right: a random binary phase mask. Spatial frequencies of up to $\pm 2f_{\text{MAX}}$ are shown where $f_{\text{MAX}} = 1/2p$ and p is the pixel pitch.

4. FOURIER PLANE PERFORMANCE MEASURES

Using Fourier optics²¹, and neglecting a leading phase factor, the light’s electric field $U(x, y)$ in the Fourier plane can be written as the scaled two-dimensional Fourier transform²² of the field $u(x', y')$ leaving the SLM:

$$U(x, y) = -\frac{i}{s} \mathcal{F}_s[u] * \mathcal{F}_s \left[\text{rect} \left(\frac{x}{W_s}, \frac{y}{W_s} \right) e^{i\phi(x, y)} \right] \quad \mathcal{F}_s[u] = \frac{1}{s} \iint u(x', y') \exp \left[-i \frac{2\pi}{s} (xx' + yy') \right] dx' dy' . \quad (1)$$

The field $U(x, y)$ is proportional to the convolution of the Fourier transform of the SLM with the Fourier transform of the phase mask. Here s is the scale factor for the particular optical system configuration, and $*$ represents the convolution integral. For a single-lens Fourier transform system in which the SLM and Fourier plane are a distance f from a lens of focal length f (Figure 4), the scale factor is $s = \lambda f$. The scale factor relates spatial frequency (f_x, f_y) in the input plane (x', y') to position in the Fourier plane: $(x, y) = (sf_x, sf_y)$. The function $\exp[i\phi(x, y)]$ represents the phase mask.

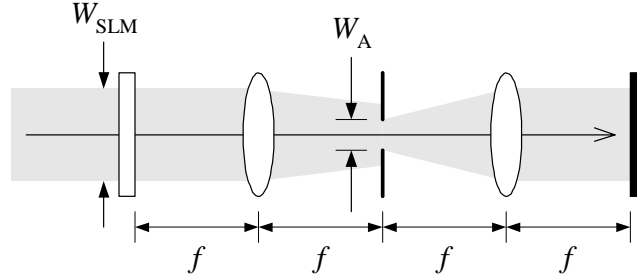


Figure 4. Illustration of a simple model for the optical path of an HDS system's read and write beam paths. The storage medium would be located at the position of the aperture. The reference beam has been omitted.

The effect of the phase mask can be seen clearly by re-writing $u(x, y)$ as the sum of two parts.

$$u(x, y) = \tilde{u}(x, y) + \bar{u} \quad \bar{u} = \frac{1}{W_{SLM}^2} \iint u(x, y) dx dy \quad (2)$$

We refer to $\tilde{u}(x, y)$ as being the AC part of $u(x, y)$ and to \bar{u} as being the DC part, W_{SLM} is the width of the square SLM. The field in the Fourier plane can now also be written as the sum of two parts.

$$\begin{aligned} U(x, y) &= -\frac{i}{s} \bar{u} \mathcal{F}_s[PM] - \frac{i}{s} \mathcal{F}_s[\tilde{u}] * \mathcal{F}_s[PM] \\ &\equiv U_{DC}(x, y) + U_{AC}(x, y) \end{aligned} \quad (3)$$

This expression shows that light in the Fourier plane can be understood as consisting of DC information that has been scattered to have a distribution proportional to the phase mask's transform, plus the transform of AC information that has been convolved with the Fourier transform of the phase mask. The action of the phase mask on the DC information is extreme, because it maps light from a 0-dimensional distribution (the DC spot) onto a 1 or 2-dimensional distribution. The phase mask's effect on AC information is less dramatic because it merely redistributes information that was already spread out in 2-dimensions.

For high fidelity recording by an HDS medium of limited dynamic range we want the amplitude distribution of the redistributed DC spot (convolved with the phase mask) to be as similar as possible to the phase-mask-redistributed AC information. Ideally, their average values would be roughly equal to one another in order to ensure that both types of information fall within the storage system's dynamic range. The function $\rho(I)$ can be used to characterize the distribution of optical power among the various light intensities I present in the Fourier plane.

$$\rho(I) = \frac{dP(I)}{dI} \quad P_T = \int_0^\infty \rho(I) dI \quad (4)$$

Here P_T is the total optical power at the Fourier plane. We can use $\rho(I)$ to determine the mean light intensities of the DC and AC light distributions, and to define a dynamic range performance metric \mathcal{R} (measured in dB) which depends on their ratio.

$$\mathcal{R} = 10 \log \left(\frac{\langle I_{DC} \rangle}{\langle I_{AC} \rangle} \right) \quad \langle I_{AC} \rangle = \frac{\int_0^\infty I \rho_{AC}(I) dI}{\int_0^\infty \rho_{AC}(I) dI} \quad \langle I_{DC} \rangle = \frac{\int_0^\infty I \rho_{DC}(I) dI}{\int_0^\infty \rho_{DC}(I) dI} \quad (5)$$

Here I_{DC} refers to $|U_{DC}|^2$ and I_{AC} refers to $|U_{AC}|^2$. Of course the real Fourier plane light intensity is proportional $|U_{AC} + U_{DC}|^2$, but I_{DC} and I_{AC} nevertheless serve our purpose of comparing the relative amplitudes of redistributed AC and DC information. In the case of no phase mask we have $\langle I_{DC} \rangle \cong N^2 \langle I_{AC} \rangle$ and we have $\mathcal{R} \cong 10 \log N^2$ (60dB for a 1,000×1,000 SLM). As a phase mask becomes more and more effective its \mathcal{R} value decreases. In the case of perfect hot spot suppression we would have $\langle I_{DC} \rangle \cong \langle I_{AC} \rangle$ and so $\mathcal{R} \cong 0$ dB. The goal of the phase mask design is to produce an \mathcal{R} value that falls within the capabilities of the storage system, e.g. if the storage system dynamic range is 30dB then we want $\mathcal{R} \leq 30$ dB. As will be shown, making \mathcal{R} smaller than necessary may not be desirable because of its effect on interpixel crosstalk.

Figure 5 shows dynamic range values \mathcal{R} calculated for a range of phase slopes Δ . Masks with larger values of Δ distribute DC energy over larger areas and are more effective at attenuating the hot spot. Fourier-plane light intensities were computed for a 100×100 pixel SLM whose pixels were set to randomly selected values of 0 or 1. The width of the Fourier plane region included in the computations was equal to $5s/p$, i.e. 5 times the width of the 1st-order diffraction pattern. Computations were done for an SLM whose pixel width w is equal to its pitch p (100% fill factor), i.e. $w/p = 1$. Although not shown, \mathcal{R} values decrease for small pixel fill factors. Whether for AC or DC, the mean values of the power distribution can be shown to be equal to $\langle I \rangle = \frac{\sum_{i,j} I_{ij}^2}{\sum_{i,j} I_{ij}}$ where the I_{ij} values are intensity samples in the Fourier plane. Recall that $\langle I_{AC} \rangle$ and $\langle I_{DC} \rangle$ are averages of the power distribution functions $\rho_{AC}(I)$ and $\rho_{DC}(I)$; they are not areal averages in the Fourier plane.

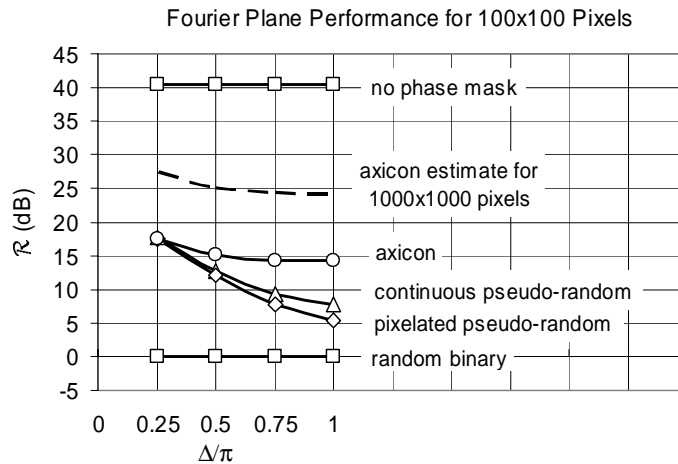


Figure 5. Calculated dynamic range values \mathcal{R} for a range of phase slopes, four types of phase masks, and for an SLM without a phase mask. These values were computed for 100×100 pixel SLMs, an estimated axicon curve for 1000×1000 pixel SLMs is shown for comparison. Only the axicon and no-mask curves depend on SLM size.

It is apparent (and no surprise) that the random binary phase mask with $\mathcal{R} \cong 0$ dB is the most effective for reducing the brightness of the DC hot spot. The pixelated pseudo-random phase mask is only slightly more effective than its non-pixelated counterpart. The benefit of not needing to align the continuous phase mask with the SLM's pixels seems to come at very little cost to performance. The axicon is the weakest performer – unlike the other mask types its effectiveness goes down (\mathcal{R} gets larger) as the number of pixels in the SLM grows: $\mathcal{R} \sim 10 \log N$. However, the ability of the phase mask to reduce the Fourier transform's dynamic range is only one consideration. We also need to understand how phase masks affect interpixel crosstalk in the recalled image of the SLM.

5. OUTPUT IMAGE PERFORMANCE MEASURES

Again using Fourier optics, the electric field of the recalled wave front can be written as a convolution of the input field $u(x,y)\exp[i\phi(x,y)]$ with a sinc function that is the Fourier transform of a square aperture of width W_A .

$$u'(x,y) = -\frac{\alpha^2}{p^2} \text{sinc}\left(\alpha \frac{x}{p}, \alpha \frac{y}{p}\right) * u(-x,-y) e^{i\phi(-x,-y)} \quad \alpha = \frac{pW_A}{s} \quad (6)$$

The ratio α relates the width of the Fourier plane aperture W_A (\sim width of the hologram) to the width of the Fourier transform. The highest spatial frequency present in the SLM data f_{MAX} is equal to $1/2p$ where p is the SLM's pixel pitch; at $\alpha = 1$ the hologram aperture is just large enough to pass light corresponding to f_{MAX} .

Figure 6 shows simulations of a recalled data page as the Fourier plane aperture shrinks from $\alpha = 10$ to $\alpha = 1$ (the ratio of pixel width to pitch is 0.9 in this example). At $\alpha = 10$ it is easy to distinguish between ON and OFF pixels. At $\alpha = 1$, however, it looks as though it may no longer be possible to distinguish between the ON and OFF states due to severe interpixel crosstalk. Note that this simulation does not include additional degradation that might be caused by storage medium imperfections (e.g. dynamic range limits) or by other HDS system imperfections. In order to maximize data storage density, the Fourier plane aperture size α might be set to the smallest possible value that allows discrimination of ON and OFF states. What is the minimum value of α that allows accurate discrimination between ON and OFF pixels? How is the minimum useful aperture size affected by the presence of a phase mask?

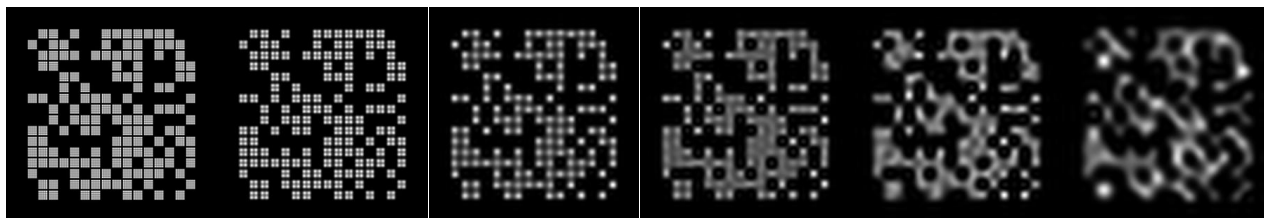


Figure 6. Computed examples of recalled images of a 16×16 pixel data pattern for Fourier plane aperture sizes of $\alpha = 10, 5, 2, 1.67, 1.33, 1.0$. The ratio of pixel width to pitch is 0.9. This is without a phase mask.

To answer the above questions we first look at histograms of pixel brightness. We assume that the SLM is viewed by an image sensor (camera) whose pixel pitch and width exactly match that of the SLM. Signal levels for individual camera pixels are computed by integrating the spatially varying light intensities falling on their apertures, with a spatial resolution ranging from $1/10$ to $1/15$ of a pixel pitch. Histograms of camera pixel signals are shown in Figure 7 for a 128×128 pixel system with no phase mask.

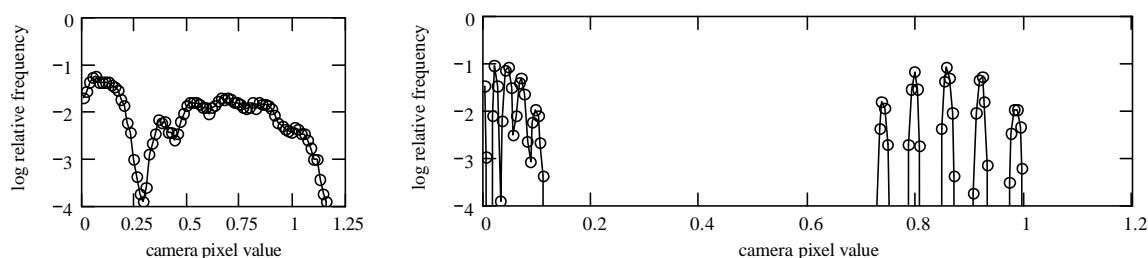


Figure 7. Histograms of camera signals computed for two Fourier plane aperture sizes. The SLM and camera each contain 128×128 pixels with $w/p = 1$. Left: $\alpha = 1$. Right: $\alpha = 2$.

The ON and OFF pixels are easily distinguished from one another at an aperture size of $\alpha = 2$ and they are just barely distinguishable at $\alpha = 1$. In order to distinguish ON from OFF we require that the minimum ON signal seen by the camera be greater than the maximum OFF signal. Figure 8 shows computed minimum-1 (minimum ON) and maximum-0 (maximum OFF) signals for a range of Fourier plane aperture sizes α , and with and without a random binary phase mask. Without a phase mask the maximum-0 and minimum-1 curves cross at $\alpha = 1$. This is the aperture

size that is just large enough to pass the highest spatial frequency present in the data ($f_{MAX} = 1/2p$). Adding the phase mask increases interpixel crosstalk. To offset the increased crosstalk we must use a larger Fourier plane aperture, as illustrated by the fact that the maximum-0 and minimum-1 curves cross at a larger value of α in this case.

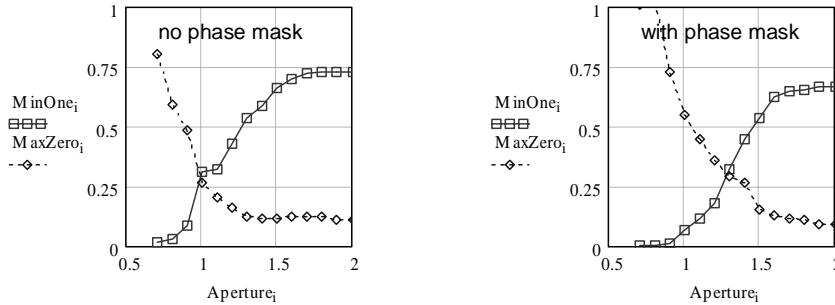


Figure 8. Curves of minimum-1 and maximum-0 vs. aperture α with no phase mask (left) and with a random binary phase mask (right). The calculations are for a 64×64 pixel SLM with $w/p = 1$.

For each type of phase mask and for a range of phase slopes Δ we can use curves such as shown in Figure 8 to determine the minimum aperture size required for a bit-error-rate (BER) of 0, i.e. the smallest aperture that allows us to accurately distinguish between ON and OFF pixels in each case. Figure 9 shows computed minimum α 's for the phase masks considered here (for a 100×100 SLM). Since larger values of α mean that a larger Fourier plane aperture is needed, we might conclude that smaller values of α are best because they allow for higher data storage densities.

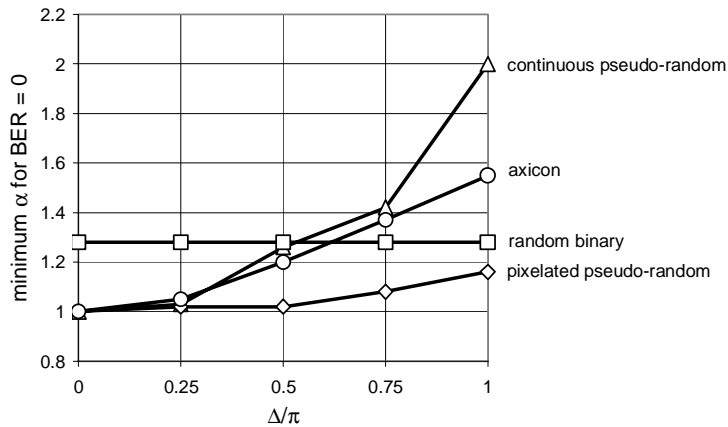


Figure 9. These curves show the minimum aperture size α needed to distinguish 1's from 0's as the phase mask's maximum phase change per pixel Δ is varied. The value $\Delta = 0$ corresponds to no phase mask. The random binary phase mask is shown for reference, it is independent of Δ . The SLM size is 100×100 .

Assuming that each pixel of the SLM represents 1-bit of data, the data density σ in the Fourier plane is given by $\sigma = N^2/W_A^2$ where $W_A = \alpha s/p$ is the area of the minimum Fourier plane aperture needed to distinguish 1's from 0's. Recalling that the SLM width is $W_{SLM} = Np$ we can write the following expression for data density.

$$\sigma = \frac{W_{SLM}^2}{\alpha^2 s^2} \quad \frac{\sigma}{\sigma_1} = \frac{1}{\alpha^2} \quad (7)$$

Here σ_1 is the data density at $\alpha = 1$. Figure 10 shows the data of Figure 9 re-plotted as σ/σ_1 vs. Δ in order to show the tradeoff between data storage density and phase mask "strength" (recall that larger Δ 's produce smaller \mathcal{R} 's). Apart from the random binary phase mask, the pixelated pseudo-random phase mask shows the least penalty in storage density while the continuous pseudo-random phase mask and axicon show the greatest penalty.

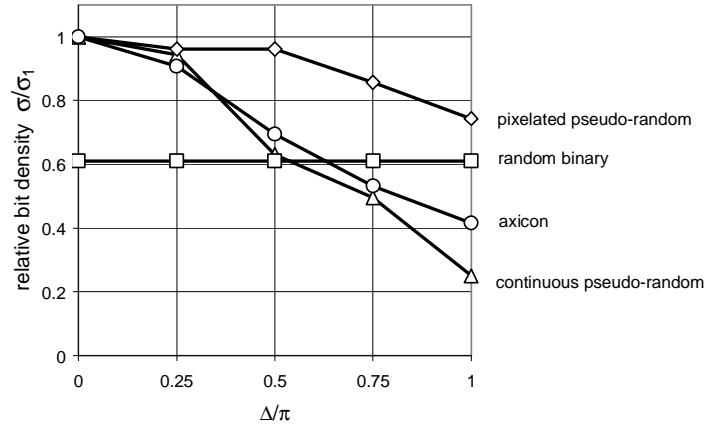


Figure 10. These curves show reductions in data density caused by enhanced interpixel crosstalk as the phase mask's maximum phase change per pixel Δ increases. The value $\Delta = 0$ corresponds to no phase mask. The random binary phase mask is shown for reference – it does not depend on Δ . Curves are independent of N .

6. FOURIER PLANE/OUTPUT PLANE TRADEOFFS

In previous sections we've described separate phase mask performance measures for the Fourier plane and the output plane. By combining the bit density vs. Δ data of Figure 10 with the \mathcal{R} vs. Δ data of Figure 5 we can eliminate Δ to produce plots of bit density vs. dynamic range \mathcal{R} . The resulting curves are shown in Figure 11. In general, for $\mathcal{R} > \sim 3\text{dB}$, we see that pixelated pseudo-random phase masks allow for the highest bit density while axicons have the lowest bit density. Unlike curves for the other phase masks, axicon performance becomes poorer as the size N of the SLM increases.

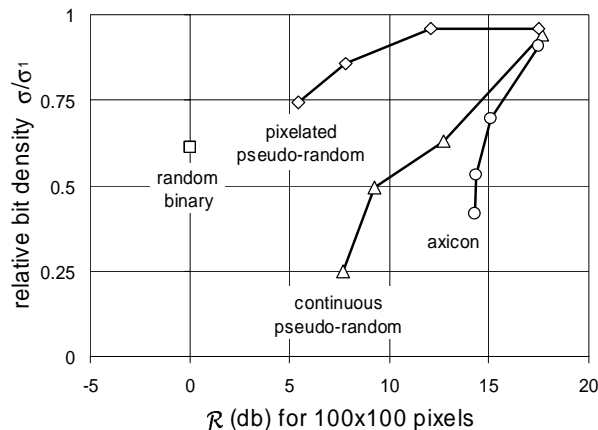


Figure 11. Plots of data storage density vs. Fourier plane dynamic range \mathcal{R} for an SLM size of 100×100 . The \mathcal{R} value of the axicon increases as $10 \log N$, \mathcal{R} values of the other mask types are independent of N .

Given the dynamic range limit of a particular HDS system, Figure 11 can be used to determine which phase mask types can be used. For example, suppose that the mean light intensity of DC information in the Fourier plane must be no more than 10 times brighter than the AC information (this limits us to $\mathcal{R} \leq 10\text{dB}$) and that we want $\sigma/\sigma_1 > 0.75$. Only the pixelated pseudo-random phase mask satisfies these requirements. If the HDS dynamic range were instead greater than about 16dB then any phase mask type other than random binary could be used, at least for an SLM size of 100×100 . If we were considering a 1000×1000 SLM then the axicon curve would shift to the right by 10dB ($\mathcal{R}_{\text{AXICON}} \sim 10 \log N$), so an axicon could only be used in HDS systems having a dynamic range greater than about 26dB. Although not shown here, \mathcal{R} values decrease for pixel fill factors of less than 100% ($w/p < 1$).

7. GRAY SCALE CONSIDERATIONS

So far we've considered only HDS systems which encode one bit of data per pixel. If the SLM pixels are capable of multiple modulation states (e.g. gray scale) then each pixel can represent more than 1-bit of data, potentially increasing data storage density. Figure 12 (no phase mask) shows histograms of camera pixel signals computed for $\alpha = 1$ and for two pixel sizes, $w/p = 1$ and $w/p = 0.5$. Each SLM pixel was randomly set to one of four equally spaced intensity values (0, 1/3, 2/3, 1). We see that although an aperture size of $\alpha = 1$ was sufficient to distinguish two states (ON and OFF), it is insufficient to distinguish more than two states unless the pixel fill factor is reduced. The penalty for reducing w/p to 0.5 in a system with matching SLM and camera is that optical throughput drops to $(1/2)^2 \times (1/2)^2 = 1/16$ of the 100% fill factor case. The alternative is to increase the size of the Fourier plane aperture, the penalty being some loss in storage density.

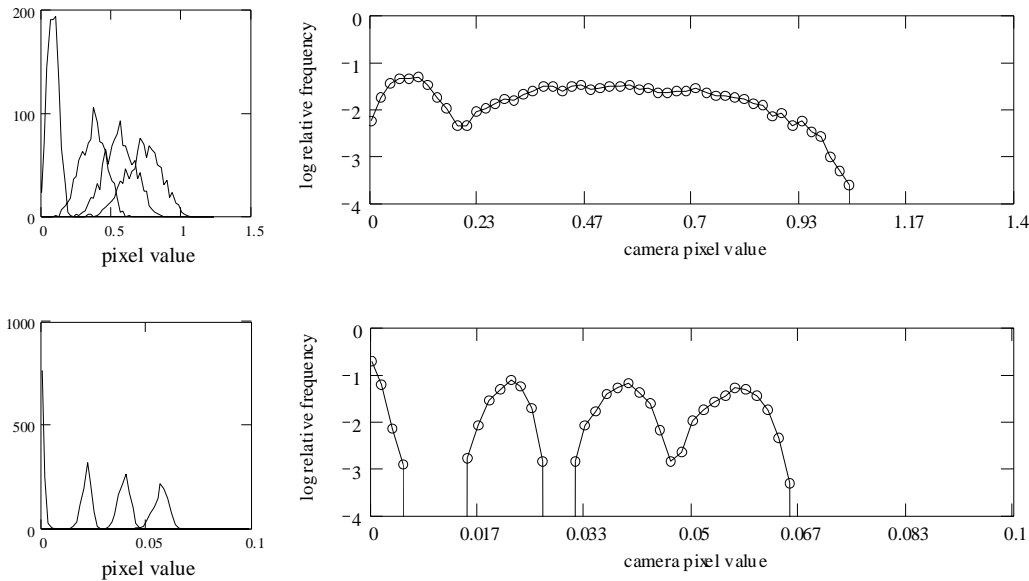


Figure 12. Computed histograms of camera pixel signals for a 64×64 SLM and camera in a two-bit per pixel HDS system. The top two plots are for a pixel size of $w/p = 1$. Top left shows individual histograms for the four input signal levels, top right shows the undivided histogram of signals. The lower plots are for a pixel size of $w/p = 0.5$.

8. SUMMARY

Performance metrics have been defined here which allow quantitative comparisons of phase mask designs, and which show tradeoffs that must be considered when selecting which mask type to use in an HDS system. In particular, these metrics show that reduced dynamic range in the Fourier plane comes at the cost of reduced data storage density. The storage density penalty can be lessened by reducing the pixel fill factor $(w/p)^2$, this however trades increased storage density for reduced optical throughput and signal-to-noise ratio. The use of gray scale in an SLM requires a larger Fourier plane aperture size (lowering storage density, at least partially offsetting gains from using gray scale) or reductions in fill factor.

A topic not yet considered is data-dependent phase mask performance. For example, when using a binary phase mask with a 1-bit-per-pixel SLM there will always be exactly one data pattern whose Fourier transform is completely unaffected by the mask (i.e. no hot spot suppression), and many patterns that are only weakly affected. System designs must take this into account to ensure that worst case data pages do not have an unacceptably high bit error rate.

ACKNOWLEDGEMENTS

This work was funded in part by NASA Phase I SBIR contract NAS2-03129, in part by NIST ATP award number 70NANB3H3031, and in part by Displaytech IR&D funds. The author thanks Mark Handschy for helpful discussions.

REFERENCES

1. Burckhardt, C.B., "Use of a Random Phase Mask for the Recording of Fourier Transform Holograms of Data Masks," *Applied Optics*, **9**(3): p. 695-700 (1970).
2. Hill, B., "Some Aspects of a Large Capacity Holographic Memory," *Applied Optics*, **11**(1): p. 182-191 (1972).
3. Stewart, W.C., A.H. Firester, and E.C. Fox, "Random Phase Data Masks; Fabrication Tolerances and Advantages of Four Phase Level Masks," *Applied Optics*, **11**(3): p. 604-608 (1972).
4. Dallas, W.J., "Deterministic Diffusers for Holography," *Applied Optics*, **12**(6): p. 1179-1187 (1973).
5. Abe, M., A. Oride, and F. Okouchi, *Phase mask for use in holographic apparatus*, US Patent 3,995,948 (1976).
6. Esaev, D.G., A.A. Lorei, and S.P. Sinita, "Continuous random phase mask," *Soviet Physics - Technical Physics*, **22**(9): p. 1150-1152 (1977).
7. Levin, V.Y., E.F. Pen, I.S. Soldatenkov, V.V. Soldatenkova, and S.I. Soskin, "Fabrication and testing of phase masks for information storage and processing devices," *Soviet Journal of Optical Technology*, **45**(3): p. 171-174 (1978).
8. Verbovetskii, A.A., N.A. Genkina, V.B. Federov, E.V. Shitova, and V.N. Kryukova, "Randomizing phase mask for recording Fourier holograms of paraphase-coded binary data," *Optics and Spectroscopy*, **45**(5): p. 810-812 (1978).
9. Iwamoto, A., "Artificial diffuser for Fourier transform hologram recording," *Applied Optics*, **19**(2): p. 215-221 (1980).
10. Akaev, A. and T. Kerimkulov, "New experimental results on the efficiency of a random phase mask in holographic memories," *Optics and Spectroscopy*, **51**(3): p. 296-299 (1981).
11. Nakayama, Y. and M. Kato, "Linear recording of Fourier transform holograms using a pseudorandom diffuser," *Applied Optics*, **21**(8): p. 1410-1418 (1982).
12. Mityakov, V.G. and V.B. Federov, "Comparison of phase masking methods in holographic recording of binary code transparencies," *Optics and Spectroscopy*, **57**(2): p. 184-188 (1984).
13. Gao, Q. and R. Kostuk, "Improvement to holographic digital data-storage systems with random and pseudorandom phase masks," *Applied Optics*, **36**(20): p. 4853-4861 (1997).
14. Bernal, M.-P., G.W. Burr, H. Coufal, J.A. Hoffnagle, C.M. Jefferson, R.M. Macfarlane, R.M. Shelby, and M. Quintanilla, "Experimental study of the effects of a six-level phase mask on a digital holographic storage system," *Applied Optics*, **37**(11): p. 2094-2101 (1998).
15. Yang, J., L.M. Bernardo, and Y.-S. Bae, "Improving holographic data storage by use of an optimized phase mask," *Applied Optics*, **38**(26): p. 5641-5645 (1999).
16. Bernal, M.-P., H.J. Coufal, R.K. Grygier, C.M. Jefferson, E. Oesterschoze, and K.F. Walsh, *Phase shifting element for optical information processing storing systems*, US Patent 6,281,993 (2001).
17. Hong, J., I. McMichael, and J. Ma, "Influence of phase masks on cross talk in holographic memory," *Optics Letters*, **21**(20): p. 1694-1696 (1996).
18. Bernal, M.-P., G.W. Burr, H. Coufal, R.K. Grygier, J.A. Hoffnagle, C.M. Jefferson, E. Oestersschulze, R.M. Shelby, G.T. Sincerbox, and M. Quintanilla, "Effects of multilevel phase masks on interpixel cross talk in digital holographic storage," *Applied Optics*, **36**(14): p. 3107-3115 (1997).
19. NIST ATP award number 70NANB3H3031 "Technologies for Advanced Holographic Data Storage", a Joint Venture with InPhase Technologies.
20. Coufal, H.J., D. Psaltis, and G.T. Sincerbox, *Holographic Data Storage*. Optical Sciences. Springer.2000.
21. Goodman, J.W., *Introduction to Fourier Optics*. Second ed. The McGraw-Hill Companies, Inc.1996.
22. O'Callaghan, M.J. and S.H. Perlmutter, "Serial transform optical correlator design principles," *Applied Optics*, **40**(20): p. 3311-3317 (2001).